Chemistry of Porphyrin-Appended Cellulose Strands with a Helical Structure: Spectroscopy, Electrochemistry, and in situ Circular Dichroism Spectroelectrochemistry

Franz X. Redl,[a, b] **Michaela Lutz,**[a] **and Jörg Daub***[a]

Abstract: Around 100 porphyrin units have been selectively linked at C(6)−O to a cellulose (Avicel®). The properties of the metal-free and zincated porphyrin-celluloses **2** and **Zn-2** have been determined by optical and electrochemical methods. Circular dichroism indicates a helical arrangement of the porphyrin units and reveals intra-chain coupling reminiscent, in the broadest sense, of strands of nucleic acids. Cyclic voltammetry and spectroelectrochemistry have been used to characterize the radical ions and dianions. The electrochromism of the oxidation of cellulose **2** to porphyrin radical cations of **2** has been employed for both molecular switching and the transduction of an electrochemical input into chiroptical signal expression.

Keywords: cellulose · circular dichroism · helical structures · in situ spectroelectrochemistry · porphyrinoids

Introduction

Dye-functionalized cellulose[1] represents an interesting target system for expressing the optical, electronic, and photophysical properties of multichromophore assemblies organized along a strictly regular chain of β(1–4)-linked D-anhydroglucopyranose units (AGU).[2–7] When, for example, the polymeric chain comprises around 200 AGUs, the length of a single strand would be about 100 nm,[8] and if every other AGU were functionalized, a total of about 100 dye units per molecule would be bound. Here, we focus on porphyrin-modified cellulose and make use of the porphyrin chromophore as a photo- and electrosensitive unit.[9–11]

Porphyrin chemistry[12] is important in various areas of research, such as analytical chemistry,[13] synthetic chemistry,[14–16] medical applications,[17–20] biochemistry and biomimetics,[21–23] materials science[24] including molecular electronics,[25, 26] and molecular information storage.[27] Porphyrins are involved in diverse functions, such as energy transfer, electron transfer, oxygen transport, and catalysis.[28] Porphyrins are present in the antenna system of photosynthesis,[29] as functional entities in redox enzymes (such as cytochrome P450 monooxygenase),[30] as well as in devices or supramolecular units,[31–36] including light-emitting systems, molecular receptors, and sensors.[37–43] Electronic coupling between porphyrins is a fundamental requirement for vectorial communication and signal transduction. Studies on dimeric,[44–49] trimeric,[50–52] and oligomeric[53–56] porphyrins and their intramolecular ππ-interactions are well established.

Porphyrins per se are achiral, but they become chiral upon stepwise symmetry breaking,[57, 58] which may either be due to a "chiral" environment or to chiral substituents.[59–61] As a result, porphyrinoid systems become chiral if they are threaded in either a clockwise or a counterclockwise twist. This is, of course, reminiscent of DNA, in which the bases are also ordered in a "spiral-staircase-type" fashion; this leads to a chiral strand that self-assembles to double-stranded DNA. Is there any evidence that helical arrays of porphyrins can be assembled along a cellulose scaffold?

Natural cellulose adopts a nanoarchitecture of great complexity and can be classified as cellulose I, II, III, or IV.[3, 6, 8] Hydrogen bonding substantially reduces its solubility. With the discovery of nonderivatizable solvent mixtures, such as dimethyl acetamide/lithium chloride,[62, 63] soluble cellulose became accessible, and thereafter cellulose derivatives with good solubility could easily be obtained.[1, 5, 8, 64, 65]

Cellulose possesses chiral carbon centers and helical chirality; furthermore, the helical strands are bundled in the solid state as a result of a hydrogen-bonded molecular architecture. The pitch of these helices amounts to about 10 Å, which is equivalent to two glucose residues (2/1 helix). Recently, work on azulene-modified cellulose[1] led us to

---

[a] Prof. Dr. J. Daub, Dr. F. X. Redl, M. Lutz
Institute of Organic Chemistry, Regensburg University
Universitätsstrasse 31, 93040 Regensburg (Germany)
Fax: (+49) 941-9434984
E-mail: joerg.daub@chemie.uni-regensburg.de

[b] Dr. F. X. Redl
Present address:
Dept. of Applied Physics and Applied Mathematics
Columbia University, New York (USA)

0947-6539/01/0724-5350 $ 17.50+.50/0

postulate helically distorted azulene dimers. We now extend these investigations to porphyrin-containing cellulose, since it is well established that porphyrins are versatile reporter groups for the stereochemistry of π–π interactions and thus for chirality. Porphyrinic acid derivatives derived from **1a** [5-(4-carboxyphenyl)-10,15,20-triphenylporphyrin] were selected as molecular probes, since they give rise to an intense ($\varepsilon_{max} \approx 400000$) Soret band at about 420 nm; this enables the study of exciton coupling[66, 67] that results from the effective transition moment B_x' (Scheme 1).[43, 68–74] It is well established that interchromophoric interactions up to about 50 Å can be observed.

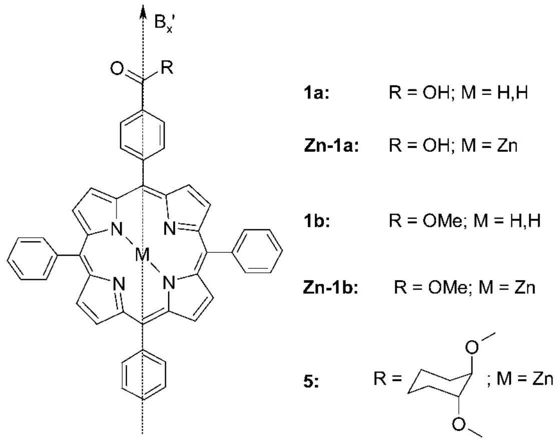

Scheme 1. Structures of the porphyrins.

Results and Discussion

The syntheses of the porphyrin-cellulose **2** and the corresponding zinc(II) complex **Zn-2** were accomplished in a multistep sequence starting from Avicel®PH101 (molecular weight around 40 kDa, 230 AGU, average particle size = 50 μm). Spectroscopic and electrochemical methods were employed in order to specify structure and function, especially with respect to porphyrin–porphyrin π-π interactions.

The syntheses of celluloses **2** and **Zn-2** were carried out according to the methodology that we used previously (Scheme 2). 2,3-Di-*O*-methylcellulose **3** was prepared from Avicel® according to a known protocol.[68, 75–77] **Zn-1a** was prepared by heating **1a** in methanol/chloroform with $Zn(OAc)_2$.[9] Several esterification methods were tested. Using a cocktail of EDC, DMAP, and pentafluorophenol in THF/chloroform turned out to give the best results, furnishing porphyrin-cellulose **2** and **Zn-2** with a degree of substitution ($DS_{porphyrin}$) of 0.4.[78–80] Diverse experiments aimed at increasing the *DS* value were unsuccessful; this indicates that steric hindrance is likely to impede a higher degree of substitution. Since, as outlined below, degradation of the cellulose is negligible, around 100 porphyrin units are bound to one string of cellulose. Celluloses **2** and **Zn-2** were both found to be well soluble in THF and chloroform.

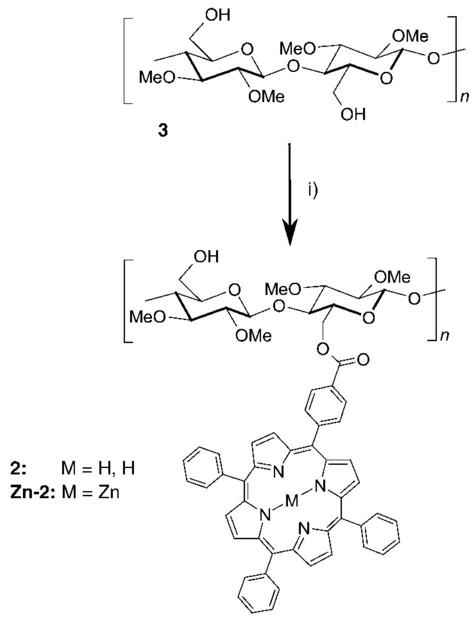

Scheme 2. Syntheses of porphyrin-celluloses **2** and **Zn-2**. i) EDC, DMAP, THF, $CHCl_3$, pentafluorophenol, **1a** or **Zn-1a**.

Abstract in German: *Die regioselektive Synthese (Ausgangsmaterial: Avicel®) liefert farbstoffmodifizierte Cellulose, derivatisiert mit etwa hundert Porphyrineinheiten pro Cellulosestrang. Die Porphyrin-Cellulose und Zink-Porphyrin-Cellulose Konjugate werden mit optischen, elektrochemischen und spektroelektrochemischen Methoden untersucht. Der Circulardichroismus belegt intramolekulares „Exciton Coupling". Eine linksgängige helikale Anordnung der Chromogene wird aus dem Vorzeichen abgeleitet. Durch in-situ-Circulardichroismus-Spektroelektrochemie wird gezeigt, dass Porphyrin-Cellulose* **2** *geeignet ist, elektrochemische Signaleingabe in chiroptische Signalausgabe zu wandeln.*

Size-exclusion chromatography: Celluloses **2** and **Zn-2** were characterized by size-exclusion chromatography on an Ultra-Styragel HR4 column (Waters) with THF as the eluent (Figure 1).

The chromatograms clearly show that both **2** and **Zn-2** are polydisperse materials. In comparison with azulene-cellulose

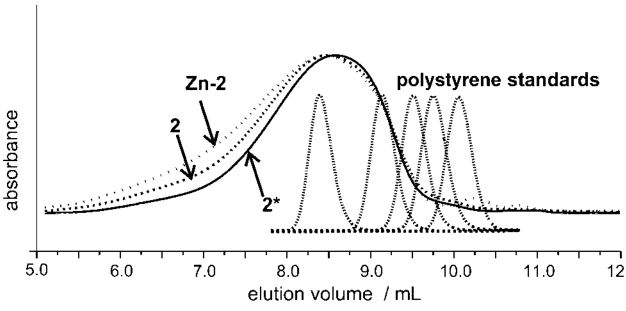

Figure 1. Gel-permeation chromatograms of porphyrin-cellulose **2** and **Zn-2**; chromatogram **2*** is from a fraction of **2** subjected to column chromatography (SiO_2, THF) beforehand; the polystyrene standards correspond to molecular weights (M_w), from left to right, of 23000, 9600, 5520, 3700, and 2340.

0947-6539/01/0724-5351 $ 17.50+.50/0

4 ($DS_{\text{azulene}} = 0.6$),[1] the half-width of the elution peak is smaller; this indicates a lower degree of aggregation[81–83] of celluloses **2** and **Zn-2**.

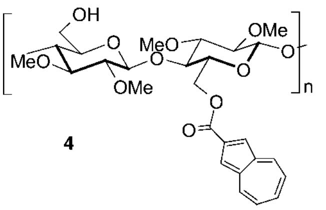

4

It is interesting to note that, compared with azulene-cellulose **4**, the porphyrin-cellulose **2** is more mobile upon chromatography on silica gel (THF as eluent); this indicates a stronger shielding of the cellulose backbone by the lipophilic porphyrin subunits. Trace **2*** in Figure 1 shows that chromatography of **2** on silica gel leads to fractionation, as indicated by the reduced fronting of the chromatogram due to the removal of that fraction of porphyrin-cellulose **2** that has a larger hydrodynamic volume. Assuming that porphyrin-cellulose **2** has a $DS_{\text{porphyrin}}$ of 0.4 and a DS_{methoxy} (at C(2)–O/C(3)–O) of 1.93,[76, 84] an average molecular weight of approximately 100 kDa seems to be reasonable.

^{1}H NMR spectroscopy: The ^{1}H NMR spectrum of **2** shows significant line broadening, as expected for a polymer (Figure 2). Based on a comparison of porphyrin-cellulose **2** and bis(porphyrin) **5** with porphyrin esters **1b**, we interpret the ^{1}H NMR spectrum of **2** in terms of a porphyrin–porphyrin stacking structure. The phenyl proton signals of bis(porphyrin) **5** and porphyrin derivative **2** show a greater range of shifts than those of **1b** and the ^{1}H NMR spectra of **2** and bis(porphyrin) **5** are rather similar. Thus, as the porphyrins in **5** are known to adopt also a staggered conformation, this may also be the case for porphyrin-cellulose **2**, as depicted in Scheme 3.

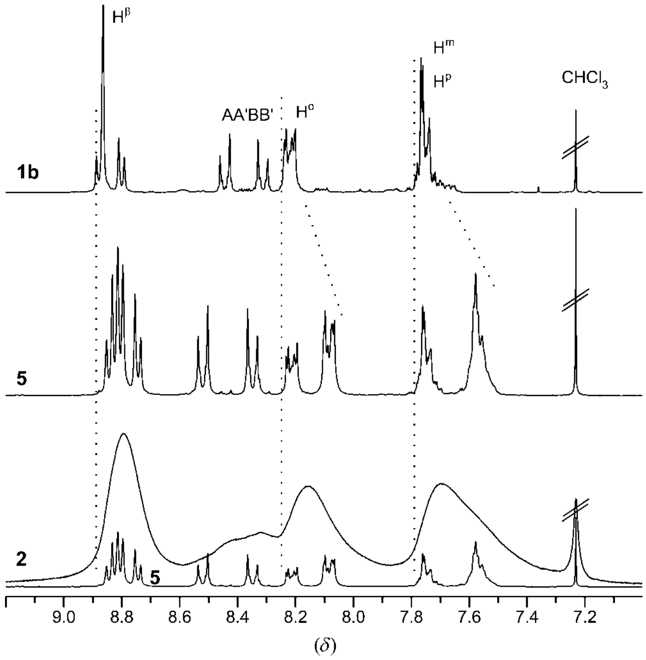

Figure 2. ^{1}H NMR spectra of methyl ester **1b**, cyclohexanediol derivative **5**, and porphyrin-cellulose **2** (250 MHz, $CDCl_3$, 24 °C). For further assignment of the signals, see Experimental Section.

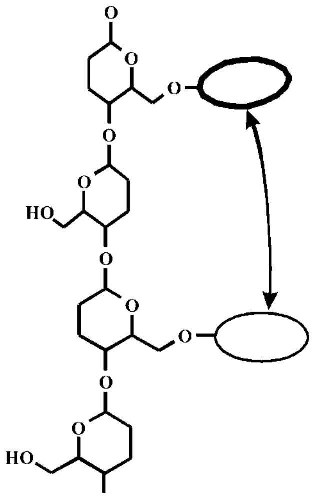

Scheme 3. Schematic representation of porphyrin-cellulose conjugate **2**, assuming functionalization at alternate AGU units.

The ^{1}H NMR spectra of the zinc(II)-porphyrin **Zn-1b**, the porphyrin-celluloses **2** and **Zn-2**, and **Zn-2**/[D$_6$]pyridine are shown in Figure 3. Line broadening is most pronounced in the spectrum of **Zn-2**; this indicates inter- or intramolecular association, which is further corroborated by the fact that the line broadening in the ^{1}H NMR spectrum of **Zn-2** is reduced on adding pyridine (third spectrum from top). It is also noteworthy that the porphyrin protons in **2** and **Zn-2**/[D$_6$]pyridine are shifted to higher field compared with those of ester **Zn-1b**; this is again consistent with neighboring porphyrin units being staggered.

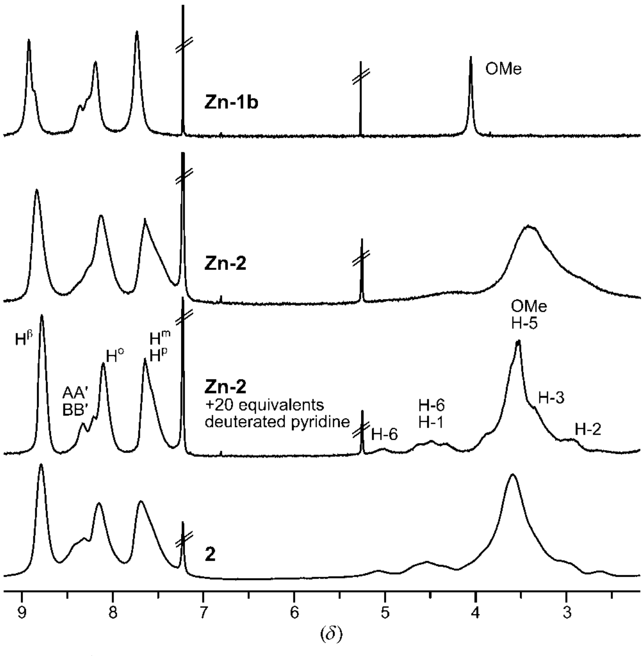

Figure 3. ^{1}H NMR spectra of (from top to bottom): methyl ester **Zn-1b**, zinc porphyrin **Zn-2**, **Zn-2**/[D$_6$]pyridine, and porphyrin-cellulose **2** (250 MHz, $CDCl_3$, room temperature).

Electronic spectra: UV/Vis and circular dichroism (CD): Electronic spectra obtained by using unpolarized or circularly polarized light are found to be a critical tool for monitoring the interaction of adjacent porphyrins. The UV/Vis spectrum of **2** (Figure 4) consists of an intense absorption band at approximately 420 nm, known as the Soret band, and five satellite bands located in the visible region between 490 and 700 nm. Figure 5 depicts the CD and absorption spectra of **2** and **Zn-2**.

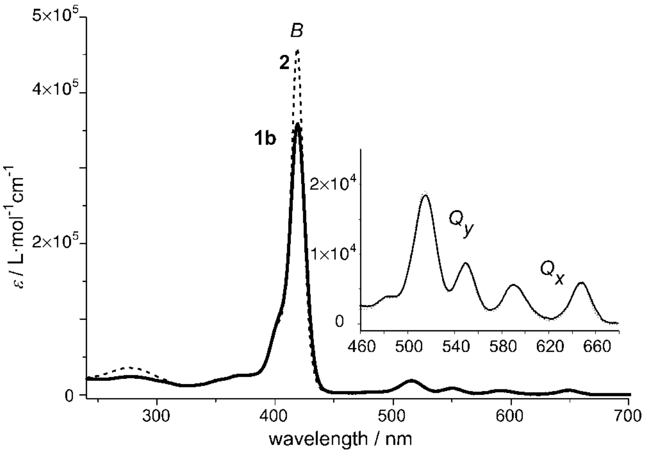

Figure 4. UV/Vis spectra of porphyrin-cellulose **2** (solid line) and porphyrin methyl ester **1b** (dashed line) ($CHCl_3$, ε values are calculated per chromophore). Inset: magnification of part of the spectrum.

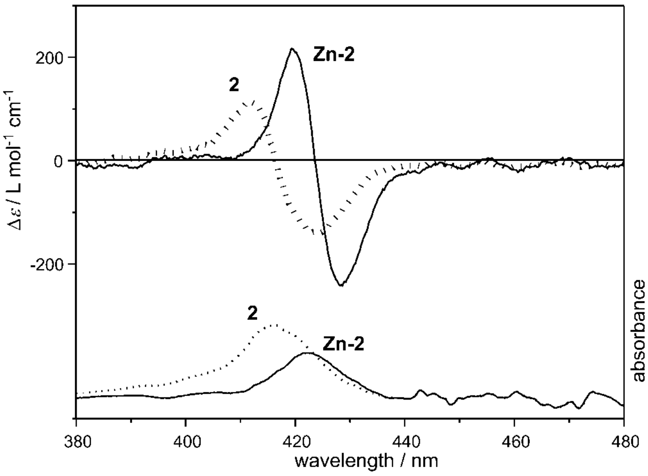

Figure 5. CD (top) and UV/Vis (bottom) spectra of porphyrin-celluloses **2** and **Zn-2** (in THF, $\Delta\varepsilon$ is quoted per chromophoric unit) both recorded with the CD spectrometer.

The UV/Vis spectra lead to the conclusion that the porphyrin moieties in **2** interact such as to result in a slightly larger half-band width of the Soret band and a reduced extinction coefficient.[46] The half-band widths in chloroform and THF are given in Table 1. In principle, three conformations of the neighboring porphyrin units are conceivable (Figure 6): a) an H-aggregate type (left), b) a tilted arrangement C (middle), or c) a J-aggregate type (right). Conformation C is in best agreement with the line shapes of the UV/Vis and CD spectra. According to Equation 1, which describes exciton splitting (ΔE)[85] of two chromophores, and assuming $\beta \approx 90°$ and $\alpha \neq$ zero, the resulting ΔE gives rise to line broadening.

Table 1. Half-band widths [cm^{-1}] of the Soret bands of compounds **1b**, **5**, **2**, **Zn-2**, and **Zn-1b**.

Solvent	**1b**	**5**	**2**	**Zn-2**	**Zn-1b**
$CHCl_3$	740	850	910	950	760
THF	750	–	1060	780	560

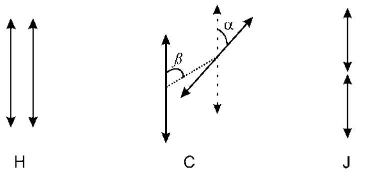

Figure 6. Types of mutual arrangement of two interacting transition moments.

$$\Delta E = \frac{2|\vec{\mu}|^2}{r^3}(\cos\alpha - \cos^2\beta) = 2V \qquad (1)$$

However, since ΔE is inversely proportional to r^3, only a small splitting is observed.

Intermolecular aggregation is evident from the UV/Vis spectra of the zinc porphyrin-cellulose **Zn-2** and the porphyrin-ester **Zn-1b** (Figure 7). Addition of methanol to **Zn-2** in $CHCl_3$ renders the solution turbid and leads to a significant decrease in the absorbance of the Soret band whilst, in contrast to **Zn-1b**, a new absorption appears at about 440 nm. Similar spectral changes are observed upon addition of methanol to porphyrin-cellulose **2** dissolved in $CHCl_3$ or THF.

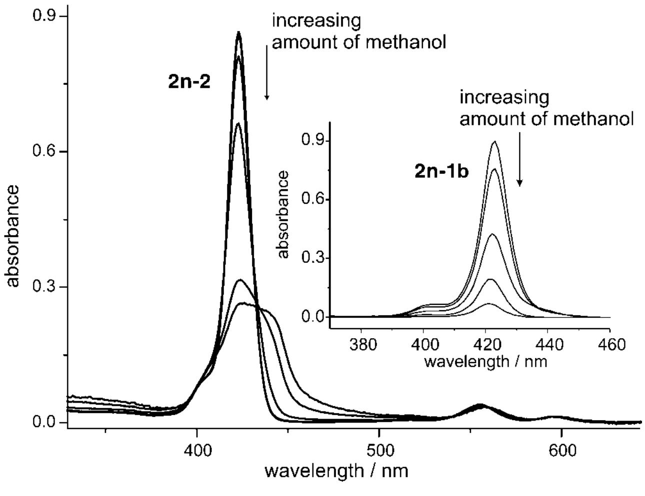

Figure 7. UV/Vis spectra of **Zn-2** and **Zn-1b** (inset) in $CHCl_3$ containing increasing amounts of methanol (the absorbencies of all the spectra of **Zn-2** are normalized with respect to the $Q(0,0)$ absorbance of **Zn-2** in $CHCl_3$; the spectra of **Zn-1b** are not normalized).

The decrease in solubility on adding methanol and, secondly, the changes that occur in the Soret band, give a strong indication of intermolecular aggregation, which may be described as an intermingling of cellulose strands comparable to the interlocking of combs.

The CD spectrum supports the concept of intramolecularly interacting porphyrins. The negative sign of the bisignate

Cotton effect is in agreement with a left-handed helical conformation (M) and a spatial arrangement of the adjacent porphyrins as depicted in Figure 8. This assignment is further supported by the fact that the degree of substitution is found to be about 0.4; which indicates that the chromophores of neighboring cellobioses interact as shown in Scheme 3 and Figure 8.

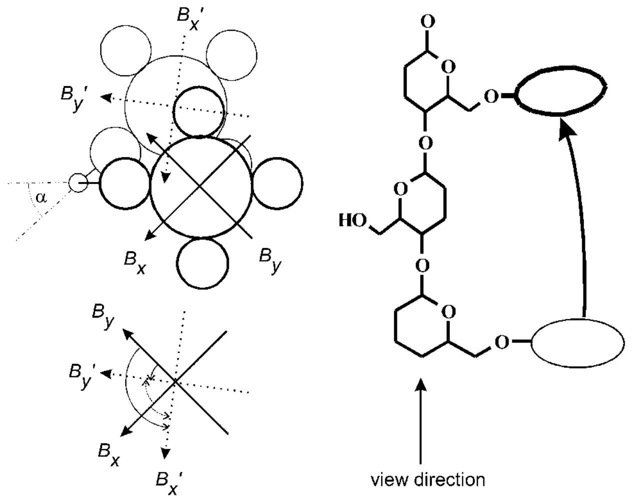

Figure 8. Schematic representation of a counterclockwise arrangement of the chromophores and the relevant transition moments of the Soret bands of porphyrins bound to alternate AGUs (composed of mutually perpendicular B_x and B_y transitions, oriented through the N-atoms).

The CD spectra (Figure 9) are also indicative of the intermolecular self-assembly of the porphyrin-cellulose **2**. If a solution of **2** in THF is added to methanol, the maximum of the band with positive sign is blue-shifted while the other is red-shifted. The structural reorganization clearly strengthens the intramolecular interaction between the porphyrin units, thus leading to an increase in the exciton splitting. Both signals are broadened; the overall shape of the couplet, however, remains unchanged. CD spectroscopy would appear to be a sensitive tool for the study of both intramolecular coupling and intermolecular aggregation.

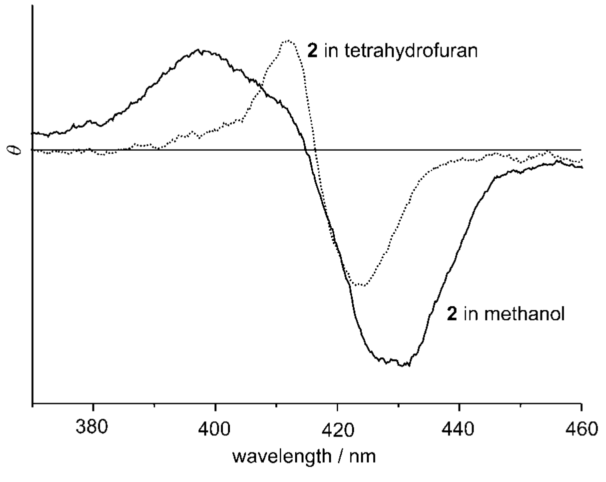

Figure 9. CD spectra of **2** in THF and in methanol/THF (prepared by dropwise addition of a solution of **2** in THF to methanol); the spectra are normalized so as to have equal absorbencies at 419 nm.

Emission spectroscopy: Excitation of **Zn-2** in THF at $\lambda_{ex} = 400$ nm leads to two emission maxima at 609 and 652 nm. Under the same conditions, with $\lambda_{ex} = 419$ nm, the emission of the zinc-free derivative **2** is red-shifted, appearing at 653 and 712 nm. The relative quantum yields of the cellulose derivatives are given in Table 2; it can be seen that the quantum yield of fluorescence of the zinc(II) complex **Zn-2** is significantly lower. Preliminary results from time-resolved measurements on **2** ($\lambda_{ex} = 347.15$ nm) yielded relative fluorescence quantum yields $\phi_F(H_2TPP)/\phi_F(\mathbf{2}) = 1.2$ and a lifetime of the excited singlet state of **2** of $\tau = 7.8$ ns. On increasing the intensity of the irradiation, the quantum yield of the fluorescence and the lifetime τ of the excited state were found to decrease; this gives a strong indication of singlet-singlet annihilation. The solvent dependency of $\phi_F(\mathbf{2})$ compared with that of $\phi_F(\mathbf{1b})$ is also remarkable. The emission of **2** in THF is clearly weaker and depends on the excitation wavelength; this can be attributed to an enhanced interaction/aggregation between the chromophores.

Table 2. Relative fluorescence quantum yields ϕ_{rel} of porphyrin compounds **1a**, **1b**, **2**, **5**, **Zn-1b**, and **Zn-2** (N_2-saturated solution, $c \approx 10^{-7}$ mol L^{-1}).

	ϕ_{rel}[a]	ϕ_{rel}[b]	ϕ_{rel}[c]	ϕ_{rel}[d]
2	1.20	0.85	0.35	0.58
1b	≡1.00	≡1.00	≡1.00	≡1.00
1a	0.97	–	–	–
5	1.01	–	–	–
Zn-1b	–	0.48	0.46	0.41
Zn-2	–	0.48	0.44	0.41

[a] $\lambda_{ex} = 419$ nm, $CHCl_3$. [b] $\lambda_{ex} = 422$ nm, THF. [c] $\lambda_{ex} = 400$ nm, THF. [d] $\lambda_{ex} = 533$ nm, THF.

Electrochemistry and spectroelectrochemistry: The electrochemical properties of compounds **1b**, **Zn-1b**, **2**, and **Zn-2** were examined by cyclic voltammetry in dry dichloromethane and THF solutions (Table 3). Figure 10 shows the cyclic voltammograms of porphyrin-cellulose **2** (in THF) and of porphyrin ester **1b** (in dichloromethane). A characteristic feature of the two compounds is that two reduction and two oxidation waves are observed in dichloromethane (Figure 10, right side), whereas two reduction waves and only one oxidation wave are seen in THF. By amperometry, it could be ascertained that this one-wave oxidation in THF corresponds to a two-electron process and is likely to be due to a fast disproportionation of the radical cation formed in the first step of the oxidation. The additional peak seen upon backscan reduction at -0.12 V (Figure 10, left side), as well as the peak separations $|E_{pc} - E_{pa}|$, which amount to 120 mV and 140 mV, respectively, are indicative of the limited stability of the dication. The two reduction waves of **2**, both of which correspond to one-electron processes, appear at $E_{1/2} = -1.62$ and -1.99 V versus Fc^+/Fc. Thus, they appear at almost the same potential as those of H_2TPP (-1.67 V; -1.98 V vs. Fc^+/Fc in CH_2Cl_2).[86] The zinc complex **Zn-2** shows reduction waves at -1.85 V and -2.29 V versus Fc^+/Fc and two one-electron oxidation waves at 0.44 V and 0.74 V. Due to the higher electron density of the porphyrin ligand, the reduction

Table 3. Half-wave potentials $E_{1/2}$ [V] and peak potential separations ΔE_p [mV] (in brackets) determined by cyclic voltammetry (all potentials vs. Fc^+/Fc, potential sweep rate 250 mV · s^{-1}, 0.1M TBAHFP).

Solvent	Compound	Oxidation 1st	Oxidation 2nd	Reduction 1st	Reduction 2nd	Reduction 3rd
CH_2Cl_2	**1b**[a]	0.57 (68)	0.89 (67)	– 1.67 (71)	– 2.00 (83)	–
	5[a]	0.54 (64)	0.85 (66)	– 1.68 (64)	– 2.00 (98)	– 2.22[h]
	2[a][e]	0.55 (76)	–	– 1.68 (50)	–	–
THF	**1b**[b]	0.70 (120)[c]	–	– 1.65 (68)	– 1.98 (62)	– 2.56 (140)[c]
	2[b]	0.73 (140)[c] – 0.12[d]	–	– 1.62 (73)	– 1.99 (81)	–
	Zn-1b[b]	0.42 (65)	0.74 (66)	– 1.86 (54)	– 2.26 (86)[c] – 1.02[d]	–
	Zn-2[b]	0.44 (59)	0.74 (65)	– 1.85 (66)	– 2.29 (200)[c] – 1.06[d]	–
CH_2Cl_2	**H_2TPP**[f]	0.52	0.82	– 1.67	– 1.98	–
CH_2Cl_2	**ZnTPP**[g]	– 0.3	–	– 1.75	–	–
THF		–	–	– 1.965	–	–

[a] Working electrode: Pt; [b] Working electrode: glassy carbon; [c] Not totally reversible; [d] Peak due to secondary product; [e] A more extensive oxidation or reduction scan was prohibited by the potential window of the solvent; [f] See ref. [86]; [g] See refs.[30,105]; [h] Irreversible process.

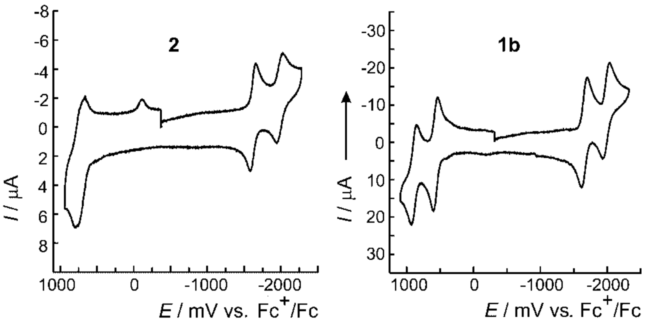

Figure 10. Cyclic voltammograms of **2** (THF) and **1b** (CH_2Cl_2, 0.1M TBAHFP, scan speed 250 mVs^{-1}).

of **Zn-2** occurs at a more negative potential relative to that of the zinc-free porphyrin **2**. The formation of the dianion of **Zn-2** at – 2.29 V appears to be accompanied by a secondary reaction. The oxidation processes of the zinc derivatives **Zn-1b** and **Zn-2** give rise to waves at less positive potentials as compared to those of **1b** and **2**. The zincated esters **Zn-1b** and **Zn-2** are both reduced at slightly greater negative potentials compared with **ZnTPP** (Table 3). The substituent effect of the ester group on the reduction is clearly negligible, and the electroreduction process is localized on the porphyrin site as a result of the minimal π-overlap between the aryl ring and the porphyrin due to the large aryl-porphyrin dihedral angle.

The electronic absorption spectra of the species generated electrochemically from **1b**, **Zn-1b**, **2**, and **Zn-2** were recorded by in situ spectroelectrochemistry with an optically transparent thin-layer electrochemical cell equipped with a gold minigrid electrode as the working electrode. Spectral data obtained from these measurements are listed in Table 4. The oxidation of the zinc-free porphyrins **1b** and **2** in dichloromethane in the potential range 0.3 – 0.65 V (vs. AgCl/Ag) leads to absorption bands in agreement with those of porphyrin radical cations (Table 4). Scanning the potential range to 1.4 V (vs. AgCl/Ag) reveals new absorption bands, which can be assigned to diprotonated porphyrin units (H_4TPP^{2+}) obtained by protonating the neutral porphyrin ligands by the electrochemically generated porphyrin dications; the latter are known to be strong acids.[87, 88]

Table 4. Absorption maxima of the compounds formed during the first reduction and oxidation processes as measured by in situ spectroelectrochemistry (0.1M TBAHFP, OTTLE).

Compound	Solvent	Absorption maxima of the species generated [nm] reduction	oxidation
1b	THF	882, 763, 687 446, 420	867, 652, 436[a]
	CH_2Cl_2	880, 762, 668, 447, 421	–
5	CH_2Cl_2	873, 782, 690, 445, 415	826, 725, 436[a]
Zn-2	THF	616, 573, 434	860, 595, 510, 448 (sh), 405, 365
Zn-1b	CH_2Cl_2	606, 564, 428	–
	DME	613, 570, 433	861, 673 (sh), 593, 443 (sh),405

[a] Not totally reversible.

Oxidation of zinc porphyrin-cellulose **Zn-2** in the range 0.75 – 1.0 V (vs. AgCl/Ag) produces the radical cation of **Zn-2** (Figure 11), which has absorption bands at 405 and 860 nm and isosbestic points at 409, 435, 539, and 565 nm.[89] The formation of the radical cation is completely reversible.

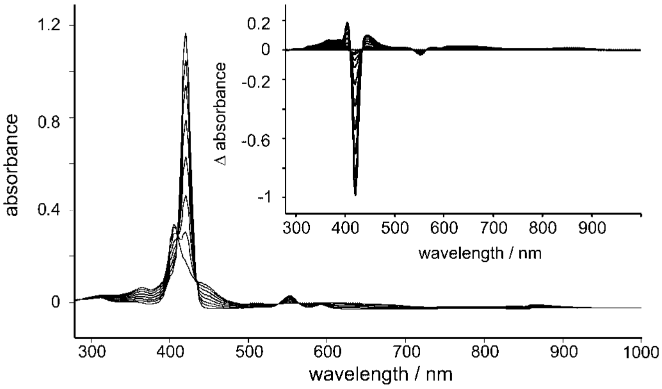

Figure 11. UV/Vis/NIR spectroelectrochemistry of the oxidation of **Zn-2** (THF, 0.1M TBAHFP, potential raised from 750 to 1000 mV vs. AgCl/Ag); inset: subtraction spectra.

On reduction of **Zn-1b** and **Zn-2** in the range – 0.9 to – 1.2 V (vs. AgCl/Ag), the strong Soret absorption at 420 nm is transformed into an intense band at 434 nm along with two red-shifted Q-bands (Figure 12). On back-scanning to – 0.9 V, the original spectrum is not completely recovered. Complete recovery can only be accomplished when the potential is scanned up to 0.4 V. Absorption bands of the radical anions (for example of **Zn-1b**$^{\bullet -}$), which were expected to be present at 455, 705, 720, and 890 nm, could not be detected, even by diode-array spectroelectrochemistry.[90–92] A comparison with

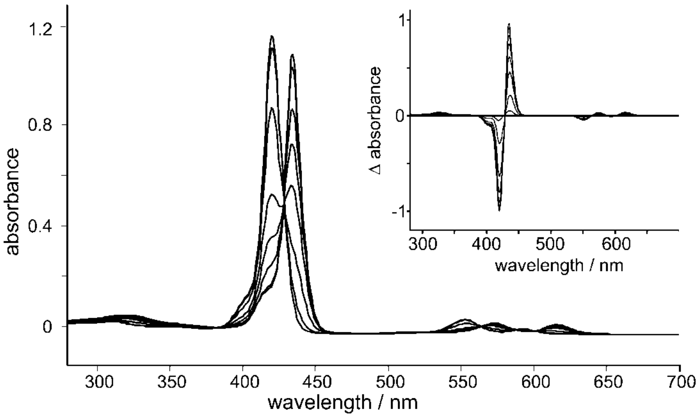

Figure 12. UV/Vis spectroelectrochemistry of the reduction of **Zn-2** (THF, 0.1M TBAHFP, potential raised from −900 to −1175 mV vs. AgCl/Ag); inset: subtraction spectra.

literature data leads to the conclusion that reduction on the spectroelectrochemistry time-scale leads directly to **Zn-1b**$^{2-}$ or the porphyrin dianions of **Zn-2**. Evidently, the intermediate radical anions are thermodynamically unstable, and the dianions and the neutral compounds are formed by disproportionation. Under the experimental conditions used, the neutral form is reduced immediately.

Chiroptical signal expression by using circular dichroism spectroelectrochemistry: CD spectroelectrochemistry is an efficient method for measuring the expression of chiroptical effects resulting from electrochemical switching.[93–97] (for a recent application, see also ref. [98]). Furthermore, CD spectroelectrochemistry may be of importance in the realm of information storage at the molecular level by virtue of its distortionless read-out based on chiropticity, or in molecular sensing.[99] Figure 13 depicts the redox switching monitored by CD. As already indicated, compound **2** shows a strongly negative CD peak in the neutral state (at $E_w = -0.2$ V vs. AgCl/Ag) at 424 nm, which vanishes completely on oxidation to the radical cation. Reduction of the radical cation restores the original CD signal. The important finding is that, in contrast to absorption spectroscopy, the CD signal disappears completely on oxidation. In other words, circular dichroism clearly represents a highly sensitive tool for probing redox switching (Figure 13).

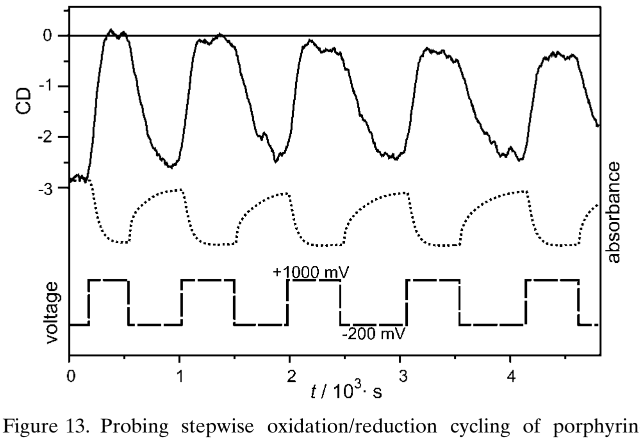

Figure 13. Probing stepwise oxidation/reduction cycling of porphyrin-cellulose **2** with square-wave voltage treatment (lower trace) and the CD band (top) or visible absorbance (middle) at 424 nm for monitoring; switching occurs between radical cation $\mathbf{2}^{\bullet+}$ and the neutral form **2** (CH_2Cl_2, 0.1M TBAHFP; potential scan between +1000 mV and −200 mV vs. AgCl/Ag).

Conclusion

In summary, we have prepared functionalized cellulose with multiple-porphyrin attachment at C(6)−O. Unlike most synthetic polymers, cellulose is chiral and has a stiff backbone with a strictly defined regiochemistry. ^{1}H NMR, UV/Vis, emission, and circular dichroism spectroscopy have been used to study the properties and the intramolecular interactions of the approximately 100 porphyrins per cellulose molecule. UV/Vis and CD spectra are clearly indicative of electronic coupling between adjacent chromophores (exciton-coupling). The Soret band absorption is broadened and yields a bisignate CD signal (CD couplet) of negative sign; this is in agreement with an (M)-helical arrangement of the cellulose-bound porphyrins. In methanol, intramolecular aggregation of the polymer strands of porphyrin-cellulose **2** is evident from the CD spectrum, which shows energetically shifted and broader absorption bands. The fluorescence quantum yield of **2** (in $CHCl_3$) is slightly higher than that of porphyrin ester **1b**. Increasing the intensity of irradiation leads to a decrease in the emission, which may be explained in terms of singlet-singlet annihilation. In dichloromethane, the celluloses **2** and **Zn-2** are reversibly reduced and reversibly oxidized with the formation of radical anions and radical cations, respectively. The spectra of the radical cations can be obtained from spectroelectrochemistry. Spectroelectrochemistry of the reduction of **Zn-1b** and **Zn-2** is consistent with the generation of the dianions expected to be formed by disproportionation.

We have also shown that polymer **2** permits electrochromism-based switching, which can be probed by absorption and circular dichroism spectroscopy. The CD couplet of **2** vanishes during the one-electron oxidation and is restored upon re-reduction. Polymer **2**, therefore, represents a chiral polymer that allows chiroptical read-out of an electrochemically induced information input.

Matching typical dye properties and typical natural polymer-based materials furnishes precursor systems for nanoscale materials with optoelectronic potential. In the present work, a functional polymer approximately 0.1 μm in size and containing about 100 porphyrin chromophores has been investigated. Cellulose per se has a typical carbohydrate-type dipole moment, which, enforced by the regular polymeric structure, gives rise to an internal electrical field of substantial strength, having the positive pole at the C(4)-terminal end and the negative pole at the C(1)-terminal end. This property can be expected to give a basis for inducing anisotropy effects, which may then be utilized in molecular assemblies and in a vectorial information (signal) flux. The helical architecture of the arrangement is expected to improve selectivity in the intermolecular interactions and in the expression of physical effects related to circularly polarized phenomena.

Experimental Section

The cellulose used in this study was AVICEL® PH101 from Fluka. The denoted *DS* values are average values determined by either ^{1}H NMR spectroscopy or elemental analysis.

UV/Vis/NIR: Perkin-Elmer Lambda 9 spectrophotometer. **IR**: BIO-RAD FTS155. **NMR**: Bruker AC250 (24 °C) and ARX400 (21 °C) spectrometers at 250/400 and 63/101 MHz for ^{1}H and ^{13}C, respectively. Chemical shifts δ (ppm) are quoted with respect to TMS (^{1}H). **Electrochemistry**: An undivided cell was used with a platinum disc as the working electrode, a platinum counter electrode, and an AgCl/Ag pseudo reference electrode. The electrochemical measurements were carried out by using a computer-controlled electrochemical apparatus consisting of an Amel System 5000 (Amel, Milan, Italy).[94,100–103] The reversible oxidation signal of ferrocenium/ferrocene (Fc^{+}/Fc) or AgCl/Ag was used as an internal reference. The solvents and the supporting electrolyte (0.1 M TBAHFP) were purified according to standard procedures.[104] All measurements were carried out under a nitrogen atmosphere. **Spectroelectrochemistry**: Solutions from the CV experiments were transferred by means of a syringe to the spectroelectrochemical cell.[94,101,103] The spectra were recorded by using a Perkin-Elmer Lambda 9 spectrophotometer. **CD spectroscopy**: Jasco J-710 spectropolarimeter; cell length 1, 0.2, 0.1 cm. **Fluorescence spectroscopy**: Hitachi F4500 fluorescence spectrophotometer. **Size-exclusion chromatography**: Instrumental set-up: Waters 717 equipped with autosampler and an Ultra-Styragel HR4 column, a Waters 2410 refractive-index detector, and a Waters 486 tunable absorbance detector. THF was used as eluent.

Preparation of porphyrin-cellulose 2 and Zn-2: General procedure: 2,3-di-*O*-methylcellulose (200 mg, ca. 1.05 mmol$_{\text{AGU}}$), 1.3 equivalents of acid (**1a** or **Zn-1a**[68]), and a fourfold excess of DMAP were suspended in anhydrous THF (20 mL) under a nitrogen atmosphere, and an equimolar amount of EDC was added at 0 °C. The suspension was stirred for five days. Thereafter, a slight excess (with respect to acid **1a** or **Zn-1a**) of pentafluorophenol was added. The solution was diluted with an equivalent volume of CHCl_3 and heated under reflux for four days. After 48 h, a further 1.5 molar excess of EDC and pentafluorophenol was added. The solution was subsequently stirred at ambient temperature for a further week. The crude product was precipitated by the dropwise addition of methanol, collected by centrifugation, and redissolved in CHCl_3. The resulting solution was filtered, and the product was precipitated by the addition of methanol. This procedure was repeated several times.

2: Yield: 170 mg (0.33 mmol, 32 %); fp: about 300 °C; ^{1}H NMR (CDCl_3, 250 MHz, TMS): $\delta = -2.79$ (NH), 2.64 (2-H$^{\text{AGU}}$), 3.04 (3-H$^{\text{AGU}}$), 3.59 (OMe$^{\text{AGU}}$, 4-H$^{\text{AGU}}$, 5-H$^{\text{AGU}}$), 4.55 (6-H$^{\text{AGU}}$, 1-H$^{\text{AGU}}$), 5.09 (6-H$^{\text{AGU}}$), 7.69 (H$^{\text{porphyrin}}$), 8.16 (H$^{\text{porphyrin}}$), 8.33 (H$^{\text{porphyrin}}$), 8.79 (H$^{\text{porphyrin}}$); IR (KBr): $\tilde{\nu} =$ 3319, 3126, 3109, 3057, 3028, 2965, 2902, 2838, 1726, 1604, 1563, 1547, 1472, 1443, 1402, 1374, 1349, 1268, 1180, 1096, 1073, 967, 801, 753, 730, 704 cm^{-1}; elemental analysis found C 68.86, H 5.69, N 5.32; *DS* (calculated from the ^{1}H NMR spectrum): 0.5, *DS* (calculated from elemental analysis): 0.43, *M* (average molecular weight per AGU, calculated from DS^{EA}): 466, *M* (average molecular weight per chromophoric unit, calculated from DS^{EA}): 1085.

Zn-2: 70 mg (0.15 mmol, 28 %); ^{1}H NMR (CDCl_3, 250 MHz, TMS, in the presence of 20 equivalents of deuterated pyridine): $\delta = 2.66$ (2-H$^{\text{AGU}}$), 2.95 (3-H$^{\text{AGU}}$), 3.39, 3.56, 3.58, 3.92 (OMe$^{\text{AGU}}$, 4-H$^{\text{AGU}}$, 5-H$^{\text{AGU}}$), 4.36, 4.52, 4.67 (6-H$^{\text{AGU}}$, 1-H$^{\text{AGU}}$), 5.04 (6-H$^{\text{AGU}}$), 7.68 (H$^{\text{porphyrin}}$), 8.14 (H$^{\text{porphyrin}}$), 8.25 (H$^{\text{porphyrin}}$), 8.36 (H$^{\text{porphyrin}}$), 8.82 (H$^{\text{porphyrin}}$); IR (KBr): $\tilde{\nu} = 3451$, 3125, 3104, 3058, 2966, 2929, 2833, 1723, 1656, 1602, 1524, 1485, 1457, 1443, 1404, 1378, 1339, 1263, 1203, 1094, 1029, 869, 802, 754, 700 cm^{-1}; *DS* (calculated from ^{1}H NMR spectrum): 0.4, *M* (average molecular weight per chromophoric unit): 1179; *M* (average molecular weight per AGU): 471.

Acknowledgement

We thank Dr. Oliver Köthe for many fruitful discussions and Dr. W. Holzer and Prof. Dr. A. Penzkofer for reporting the preliminary results of time-resolved fluorescence measurements. We are grateful to Prof. O. S. Wolfbeis for making available the CD spectrometer. Part of this work was supported by the Deutsche Forschungsgemeinschaft [Schwerpunktprogramm "Cellulose und Cellulosederivate: molekulares und supramolekulares Strukturdesign" (SPP 1011); DA 92/24–2].

[1] F. X. Redl, O. Köthe, K. Röckl, W. Bauer, J. Daub, *Macromol. Chem. Phys.* **2000**, *201*, 2091.
[2] *Macromol. Chem. Phys. Special Issue*: *Cellulose and Cellulose Derivatives*, *201* (15), **2000**.
[3] H. Krässig, *Cellulose—Structure, Accessibility, and Reactivity*, Gordon and Breach Science, Yverdon, **1993**.
[4] T. P. Nevell, S. H. Zeronian, *Cellulose Chemistry and its Applications*, Wiley, New York, **1985**.
[5] D. Klemm, B. Philipp, T. Heinze, U. Heinze, W. Wagenknecht, *Comprehensive Cellulose Chemistry—Functionalization of Cellulose*, *Vol. 2*, Wiley-VCH, Weinheim, **1998**.
[6] *Cellulose—Structural and Functional Aspects* (Eds.: J. F. Kennedy, G. O. Phillips, P. A. Williams), Ellis Horwood, Chichester, **1985**.
[7] *Cellulose Derivatives*: *Modification*, *Characterization*, *and Nanostructures*, *Vol. 668* (Eds.: T. J. Heinze, W. G. Glasser), Oxford University Press, Washington DC, **1998**.
[8] Degree of polymerization (DP) of typical cellulose materials: Cotton >3000, Ramie ≈6000–7000, cotton linters ≈800–2600, cellulose powder ≈150–300. D. Klemm, B. Philipp, T. Heinze, U. Heinze, W. Wagenknecht, *Comprehensive Cellulose Chemistry—Fundamentals and Analytical Methods*, *Vol. 1*, Wiley-VCH, Weinheim, **1998**.
[9] *Porphyrins and Metalloporphyrins—A new edition based on the original volume by J. E. Falk* (Ed.: K. M. Smith), Elsevier, Amsterdam, **1975**.
[10] *The Porphyrins, Vols. I–V* (Ed.: D. Dolphin), Academic Press, New York, **1978**.
[11] *The Porphyrin Handbook*, *Vols. 1–10* (Eds.: K. M. Kadish, K. M. Smith, R. Guilard), Academic Press, San Diego, **2000**.
[12] H. L. Anderson, *Chem. Commun.* **1999**, 2323.
[13] M. Biesaga, K. Pyrzynska, M. Trojanowicz, *Talanta* **2000**, *51*, 209.
[14] C. J. Chang, Y. Deng, C. Shi, C. K. Chang, F. C. Anson, D. G. Nocera, *Chem. Commun.* **2000**, 1355.
[15] Z. Gross, N. Galili, L. Simkhovich, *Tetrahedron Lett.* **1999**, *40*, 1571.
[16] W. Adam, V. R. Stegmann, C. R. Saha-Möller, *J. Am. Chem. Soc.* **1999**, *121*, 1879.
[17] R. Bonnett, *Chem. Soc. Rev.* **1995**, *24*, 19.
[18] E. D. Sternberg, D. Dolphin, C. Bruckner, *Tetrahedron* **1998**, *54*, 4151.
[19] T. D. Mody, *J. Porphyrins Phthalocyanines* **2000**, *4*, 362.
[20] R. K. Pandey, *J. Porphyrins Phthalocyanines* **2000**, *4*, 368.
[21] L. R. Milgrom, *The Colours of Life*, Oxford University Press, Oxford, **1997**.
[22] D. Ricard, A. Didier, M. L'Her, B. Boitrel, *ChemBioChem.* **2001**, *2*, 144.
[23] H. Kurreck, M. Huber, *Angew. Chem.* **1995**, *107*, 929, *Angew. Chem. Int. Ed. Engl.* **1995**, *34*, 849.
[24] J.-H. Chou, H. S. Nalwa, M. E. Kosal, N. A. Rakow, K. S. Suslick in *The Porphyrin Handbook—Applications*: *Past*, *Present and Future*, *Vol. 6* (Eds.: K. M. Kadish, K. M. Smith, R. Guilard), Academic Press, San Diego **2000**, p. 43.
[25] A. K. Burrell, M. R. Wasielewski, *J. Porphyrins Phthalocyanines* **2000**, *4*, 401.
[26] R. Iqbal, S. C. Moratti, A. B. Holmes, G. Yahioglu, L. R. Milgrom, F. Cacialli, J. Morgado, R. H. Friend, *J. Mater. Sci.*: *Mater. Electron.* **2000**, *11*, 97.
[27] J. Li, D. Gryko, R. B. Dabke, J. R. Diers, D. F. Bocian, W. G. Kuhr, J. S. Lindsey, *J. Org. Chem.* **2000**, *65*, 7379.
[28] B. Jiang, S. W. Yang, S. L. Bailey, L. G. Hermans, R. A. Niver, M. A. Bolcar, J. W. E. Jones, *Coord. Chem. Rev.* **1998**, *171*, 365.
[29] A. Freer, S. Prince, K. Sauer, M. Papiz, A. Hawthornthwaite-Lawless, G. McDermott, R. Cogdell, N. W. Isaacs, *Structure* **1996**, *4*, 449.
[30] T. A. Rao, B. G. Maiya, *Polyhedron* **1994**, *13*, 1863.
[31] K.-Y. Tomizaki, T. Murata, K. Kaneko, A. Miike, N. Nishino, *J. Chem. Soc. Perkin Trans. 2* **2000**, 1067.
[32] D. L. Akins, H.-R. Zhu, C. Guo, *J. Phys. Chem.* **1996**, *100*, 5420.
[33] T. Imamura, K. Fukushima, *Coord. Chem. Rev.* **2000**, *198*, 133.
[34] E. Bellacchio, R. Lauceri, S. Gurrieri, L. M. Scolaro, A. Romeo, R. Purrello, *J. Am. Chem. Soc.* **1998**, *120*, 12353.
[35] R. F. Pasternack, A. Giannetto, *J. Am. Chem. Soc.* **1991**, *113*, 7799.
[36] L. Giribabu, T. A. Rao, B. G. Maiya, *Inorg. Chem.* **1999**, *38*, 4971.

[37] Y. Kuroda, Y. Kato, T. Higashioji, J.-Y. Hasegawa, S. Kawanami, M. Takahashi, N. Shiraishi, K. Tanabe, H. Ogoshi, *J. Am. Chem. Soc.* **1995**, *117*, 10950.

[38] H. Ogoshi, T. Mizutani, *Acc. Chem. Res.* **1998**, *31*, 81.

[39] O. Rusin, V. Král, *Chem. Commun.* **1999**, 1367.

[40] J. C. Hawley, N. Bampos, R. J. Abraham, J. K. M. Sanders, *Chem. Commun.* **1998**, 661.

[41] T. Hayashi, Y. Hitomi, H. Ogoshi, *J. Am. Chem. Soc.* **1998**, *120*, 4910.

[42] T. Mizutani, K. Wada, S. Kitagawa, *J. Am. Chem. Soc.* **1999**, *121*, 11425.

[43] X. Huang, K. Nakanishi, N. Berova, *Chirality* **2000**, *12*, 237.

[44] V. V. Borovkov, J. M. Lintuluoto, M. Fujiki, Y. Inoue, *J. Am. Chem. Soc.* **2000**, *122*, 4403.

[45] V. V. Borovkov, J. M. Lintuluoto, Y. Inoue, *J. Phys. Chem. B* **1999**, *103*, 5151.

[46] M. Takeuchi, Y. Chin, T. Imada, S. Shinkai, *Chem. Commun.* **1996**, 1867.

[47] R. Shediac, M. H. B. Gray, H. T. Uyeda, R. C. Johnson, J. T. Hupp, P. J. Angiolillo, M. J. Therien, *J. Am. Chem. Soc.* **2000**, *122*, 7017.

[48] J. Fan, J. A. Whiteford, B. Olenyuk, M. D. Levin, P. J. Stang, E. B. Fleischer, *J. Am. Chem. Soc.* **1999**, *121*, 2741.

[49] T. Ema, S. Misawa, S. Nemugaki, T. Sakai, M. Utaka, *Chem. Lett.* **1997**, 487.

[50] T. Nagata, A. Osuka, K. Maruyama, *J. Am. Chem. Soc.* **1990**, *112*, 3054.

[51] A. El-Kasmi, D. Lexa, P. Maillard, M. Momenteau, J.-M. Savéant, *J. Phys. Chem.* **1993**, *97*, 6090.

[52] T. Arai, K. Takei, N. Nishino, T. Fujimoto, *Chem. Commun.* **1996**, 2133.

[53] J. Li, A. Ambroise, S. I. Yang, J. R. Diers, J. Seth, C. R. Wack, D. F. Bocian, D. Holten, J. S. Lindsey, *J. Am. Chem. Soc.* **1999**, *121*, 8927.

[54] A. Nakano, A. Osuka, I. Yamazaki, T. Yamazaki, Y. Nishimura, *Angew. Chem. Int. Ed.* **1998**, *37*, 3172.

[55] N. Aratani, A. Osuka, Y. H. Kim, D. H. Jeong, D. Kim, *Angew. Chem.* **2000**, *112*, 1517; *Angew. Chem. Int. Ed.* **2000**, *39*, 1458.

[56] J. Seth, V. Palaniappan, T. E. Johnson, S. Prathapan, J. S. Lindsey, D. F. Bocian, *J. Am. Chem. Soc.* **1994**, *116*, 10578.

[57] K. Mislow, J. Siegel, *J. Am. Chem. Soc.* **1984**, *106*, 3319.

[58] J. Daub, L. Jakob, J. Salbeck, *Chem. Ber.* **1988**, *121*, 2187.

[59] H. Kubo, T. Aida, S. Inoue, Y. Okamoto, *Chem. Commun.* **1988**, 1015.

[60] K. Konishi, Y. Takahata, T. Aida, S. Inoue, R. Kuroda, *J. Am. Chem. Soc.* **1993**, *115*, 1169.

[61] M. J. Crossley, T. W. Hambley, L. G. Mackay, A. C. Try, R. Walton, *Chem. Commun.* **1995**, 1077.

[62] C. L. McCormick, D. K. Lichatowich, *J. Polym. Sci. Polym. Lett. Edn.* **1979**, *17*, 479.

[63] C. L. McCormick, P. A. Callais, *Polymer* **1987**, *28*, 2317.

[64] A. M. Striegel, *Carbohydr. Polym.* **1998**, *34*, 267.

[65] T. Heinze, T. Liebert, *Cellulose Chem. Technol.* **1998**, *32*, 3.

[66] N. Harada, K. Nakanishi, *Circular Dichroic Spectroscopy–Exciton Coupling in Organic Stereochemistry*, University Science Books, Mill Valley, CA, **1983**.

[67] K. Nakanishi, N. Berova in *Circular Dichroism—Principles and Applications* (Eds.: K. Nakanishi, N. Berova, R. W. Woody), VCH, New York, NY, **1994**, p. 361.

[68] S. Matile, N. Berova, K. Nakanishi, J. Fleischhauer, R. W. Woody, *J. Am. Chem. Soc.* **1996**, *118*, 5198.

[69] B. H. Rickman, S. Matile, K. Nakanishi, N. Berova, *Tetrahedron* **1998**, *54*, 5041.

[70] S. Matile, N. Berova, K. Nakanishi, *Enantiomer* **1996**, *1*, 1.

[71] S. Matile, N. Berova, K. Nakanishi, *J. Am. Chem. Soc.* **1995**, *117*, 7021.

[72] X. Huang, B. Borhan, B. H. Rickman, K. Nakanishi, N. Berova, *Chem. Eur. J.* **2000**, *6*, 216.

[73] X. Huang, B. H. Rickman, B. Borhan, N. Berova, K. Nakanishi, *J. Am. Chem. Soc.* **1998**, *120*, 6185.

[74] N. Berova, B. Borhan, J. G. Dong, J. Guo, X. Huang, E. Karnaukhova, A. Kawamura, J. Lou, S. Matile, K. Nakanishi, B. Rickman, J. Su, Q. Tan, I. Zanze, *Pure Appl. Chem.* **1998**, *70*, 377.

[75] J. A. C. Gómez, U. W. Erler, D. O. Klemm, *Macromol. Chem. Phys.* **1996**, *197*, 953.

[76] T. Kondo, D. G. Gray, *Carbohydrate Res.* **1991**, *220*, 173.

[77] U. Erler, P. Mischnik, A. Stein, D. Klemm, *Polym. Bull.* **1992**, *29*, 349.

[78] G. Wendlberger, P. Stelzel, P. Thamm, E. Jaeger, *Methoden der Organischen Chemie*, *Vol. XV/2*, Georg Thieme, Stuttgart, **1974**, p. 114.

[79] G. Höfle, W. Steglich, H. Vorbrüggen, *Angew. Chem.* **1978**, *90*, 602; *Angew. Chem. Int. Ed. Engl.* **1978**, *17*, 569.

[80] K. Arai, Y. Shitara, T. Ohyama, *J. Mater. Chem.* **1996**, *6*, 11.

[81] L. Schulz, W. Burchard, R. Dönges in *Cellulose Derivatives*: *Modification*, *Characterization*, *and Nanostructures* (Eds.: T. Heinze, W. Glasser), Oxford University Press, **1998**, p. 218.

[82] L. Schulz, W. Burchard, *Papier* **1993**, *1*, 1.

[83] K. Schmidt, F.-I. Hildebrandt, P. Zugenmaier in *Polysaccharide Applications—Cosmetics and Pharmaceuticals*, *Vol. 737* (Eds.: M. A. El-Nokaly, H. A. Soini), *ACS Symposium Series*, Oxford University Press, **1999**, p. 127.

[84] O. Köthe, PhD Thesis, Regensburg University (Germany), **1999**.

[85] M. Kasha, H. R. Rawls, M. A. E.-Bayoumi, *Pure Appl. Chem.* **1965**, *11*, 371.

[86] J. H. Wilford, M. D. Archer, J. R. Bolton, T.-F. Ho, J. A. Schmidt, A. C. Weedon, *J. Phys. Chem.* **1985**, *89*, 5395.

[87] C. Inisan, J.-Y. Saillard, R. Guilard, A. Tabard, Y. L. Mest, *New J. Chem.* **1998**, 823.

[88] L. Geng, R. W. Murray, *Inorg. Chem.* **1986**, *25*, 3115.

[89] J. Fajer, D. C. Borg, A. Forman, D. Dolphin, R. H. Felton, *J. Am. Chem. Soc.* **1970**, *92*, 3451.

[90] R. H. Felton in *The Porphyrins—Physical Chemistry*, *Part C*, *Vol. 5* (Ed.: D. Dolphin), Academic Press, New York **1978**, p. 53.

[91] G. L. Closs, L. E. Closs, *J. Am. Chem. Soc.* **1963**, *85*, 818.

[92] J. Pawlik, L. Gherghel, S. Karabunarliev, M. Baumgarten, *Chem. Phys.* **1997**, *221*, 121.

[93] J. Daub, I. Aurbach, J. Salbeck, *Angew. Chem.* **1988**, *100*, 277; *Angew. Chem. Int. Ed.* **1988**, *27*, 291.

[94] J. Salbeck, I. Aurbach, J. Daub, *DECHEMA Monograph Vol. 112*, VCH, Weinheim, **1988**, p. 177.

[95] M. Porsch, G. Sigl-Seifert, J. Daub, *Adv. Mater.* **1997**, *9*, 635.

[96] C. Westermeier, H.-C. Gallmeier, M. Komma, J. Daub, *Chem. Commun.* **1999**, 2427.

[97] G. Beer, C. Niederalt, S. Grimme, J. Daub, *Angew. Chem.* **2000**, *112*, 3385; *Angew. Chem. Int. Ed.* **2000**, *39*, 3252.

[98] Y. J. Lu, Y. C. Zhu, G. J. Cheng, S. J. Dong, *Electroanalysis* **1999**, *11*, 601.

[99] a) *Molecular Switches* (Ed.: B. L. Feringa), Wiley-VCH, Weinheim, **2001**; b) B. L. Feringa, R. A. v. Delden, N. Koumura, E. M. Geertsema, *Chem. Rev.* **2000**, *100*, 1789.

[100] H. Hirschlag, Diploma Thesis, Regensburg University (Germany), **1995**.

[101] J. Salbeck, *J. Electroanal. Chem.* **1992**, *340*, 169.

[102] J. Salbeck, *Anal. Chem.* **1993**, *65*, 2169.

[103] M. Büschel, C. Stadler, C. Lambert, M. Beck, J. Daub, *J. Electroanal. Chem.* **2000**, *484*, 24.

[104] *Recommended Methods for Purification of Solvents and Tests for Impurities* (Ed.: J. F. Coetze), Pergamon, Oxford, **1983**.

[105] K. M. Kadish, J. L. Cornillon, C. L. Yao, T. Malinski, G. Gritzner, *J. Electroanal. Chem. Interfacial Electrochem.* **1987**, *235*, 189.

Received: April 17, 2001 [F3199]